Cerebral Cortex February 2012;22:455–464
doi:10.1093/cercor/bhr126
Advance Access publication June 13, 2011

Emerging Cerebral Connectivity in the Human Fetal Brain: An MR Tractography Study

Emi Takahashi[1,2,3], Rebecca D. Folkerth[4,5], Albert M. Galaburda[6] and Patricia E. Grant[1,2,3,7]

[1]Division of Newborn Medicine, Department of Medicine, Children's Hospital Boston, Harvard Medical School, Boston, MA 02115, USA, [2]Fetal-Neonatal Neuroimaging and Developmental Science Center, Children's Hospital Boston, Harvard Medical School, Boston, MA 02115, USA, [3]Athinoula A. Martinos Center for Biomedical Imaging, Massachusetts General Hospital, Harvard Medical School, Charlestown, MA 02119, USA, [4]Department of Pathology, Brigham and Women's Hospital, Harvard Medical School, Boston, MA 02115, USA, [5]Department of Pathology, Children's Hospital Boston, Harvard Medical School, Boston, MA 02115, USA, [6]Department of Neurology, Beth Israel Deaconess Medical Center, Harvard Medical School, Boston, MA 02115, USA and [7]Department of Radiology, Children's Hospital Boston, Harvard Medical School, Boston, MA 02115, USA

Address correspondence to Dr Emi Takahashi, Division of Newborn Medicine, Department of Medicine, Children's Hospital Boston, Harvard Medical School. Email: emi@nmr.mgh.harvard.edu.

Cerebral axonal connections begin to develop before birth during radial migration in each brain area. A number of theories are still actively debated regarding the link between neuronal migration, developing connectivity, and gyrification. Here, we used high angular resolution diffusion tractography on postmortem fetal human brains (postconception week (W) 17–40) to document the regression of radial and tangential organization likely to represent migration pathways and the emergence of corticocortical organization and gyrification. The dominant radial organization at W17 gradually diminished first in dorsal parieto-occipital and later in ventral frontotemporal regions with regional variation: radial organization persisted longer in the crests of gyri than at the depths of sulci. The dominant tangential organization of the ganglionic eminence at W17 also gradually disappeared by term, together with the disappearance of the ganglionic eminence. A few immature long-range association pathways were visible at W17, gradually became evident by term. Short-range corticocortical tracts emerged prior to gyrification in regions where sulci later developed. Our results suggest that the regional regression of radial organization and regional emergence of fetal brain connectivity proceeds in general from posterodorsal to anteroventral with local variations.

Keywords: brain, development, diffusion imaging, human fetus, tractography

Introduction

In the human brain, radial neuronal migration begins around the eighth gestational week (W8) (Sidman and Rakic 1973) and completes between W24 and W40, depending on brain regions (Encha-Razavi and Sonigo 2003). These migration processes are coincident with the development of corticocortical connections and gyrification as well as rapid brain growth (Rakic 1988; Caviness et al. 1996; Innocenti and Price 2005; Volpe 2008). A number of studies indicate that there are close relationships between axonal maturation and gyral formation (Goldman-Rakic and Rakic 1984; Van Essen 1997; Barbas and Rempel-Clower 1997; Hilgetag and Barbas 2005; Xu et al. 2010). In addition, a few studies have hypothesized a relationship between radial migration and gyral folding (Hilgetag and Barbas 2005). Previous studies have shown that radial glial structures regress sometime between W19 and W36, while thalamic afferent fibers grow into the cortical plate between W24 and W30 after waiting in the subplate for a period of time (Schmechel and Rakic 1979; Honig et al. 1996). This is followed by the emergence of corticocortical pathways around W30–36 (Kostovic and Rakic 1990; Kostovic and Jovanov-Milosevic 2006; Kostovic and Judas 2010). However, these studies were performed only in selected regions of the human brain (e.g., visual cortex) (e.g., Burkhalter et al. 1993; Hevner 2000) due to the technical challenges of obtaining whole-brain 3D information from postmortem specimens. Therefore, the regional variation in the loss of radial organization and development of axonal pathways in the human brain remain elusive.

In this study, we explore the potential role of high angular resolution diffusion imaging (HARDI) in studying spatiotemporal relationships of migration, developing connectivity, and gyrification in the whole brain. HARDI has been proposed to improve characterization of tissue coherence compared with diffusion tensor imaging (DTI), by defining a fiber orientation distribution function. This approach improves the ability to resolve different diffusion directions within the same voxel that result from crossing axonal bundles (Tuch et al. 2003, Leergaard et al. 2010). HARDI is effective for delineating the structural changes that occur in developing fetal (preterm) brains (Takahashi et al. 2010, 2011), in which the process of myelination is incomplete and in which crossing fibers may exist in greater numbers than in the adult brain (Innocenti and Price 2005). We have applied HARDI tractography to immature cat brains to provide whole-brain 3D visualization of developing fiber systems (Takahashi et al. 2010, 2011). Here, we apply HARDI tractography to intact whole postmortem fetal human brains between W17 and W40 to observe the tissue coherence changes that occur with development.

Experimental Procedures

Specimens

We performed MR scans on human fetal brain specimens with postconceptual ages 17, 20, 22, 24, 31, 38, and 40 weeks (W) (some of them are shown in Fig. 1). Brain samples were accrued from the Brigham and Women's Hospital and Children's Hospital Boston Departments of Pathology, under protocols approved by each hospital's institutional review board for human research. They include specimens from terminations, stillbirths, and neonatal deaths, submitted for pathologic examination after consent of parent(s) or guardian(s). A Perinatal Neuropathologist studied each sample at the time of postmortem examination,

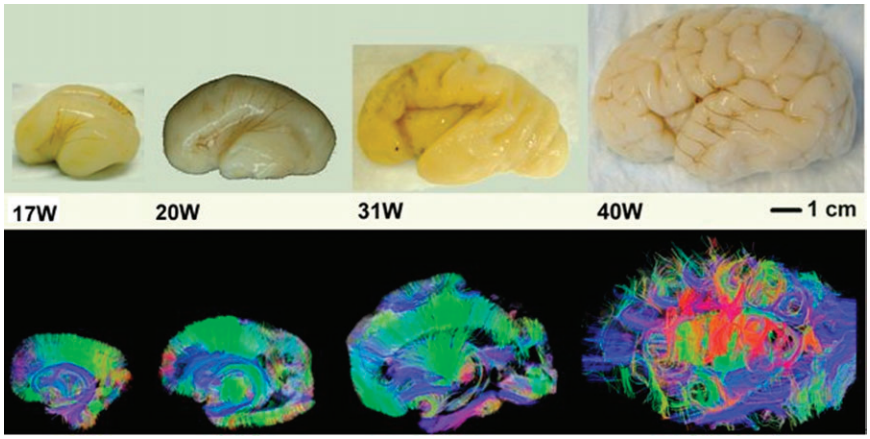

Figure 1. Pictures of fetal brains (upper row) and examples of tractography pathways that are passing through a sagittal slice (lower row) (W17, W20, W31, and W40 from the left).

and only those tissues not needed for immediate diagnosis were fixed in 4% paraformaldehyde and submitted for coded (de-identified) specimen scanning (mean fixation period was around 2–3 months). Any cases with known or suspected malformations, disruptions, or other lesions (on basis of in utero ultrasonography or postmortem findings) were excluded from this study. We scanned a total of 8 specimens across the gestational age range of the study. Brains were removed from the cranium and fixed in a 4% paraformaldehyde solution containing 1 mM gadolinium (Gd-DTPA) MRI contrast agent for at least 1 week to reduce the T_1 relaxation time while ensuring sufficient T_2-weighted signal remained. During image acquisition, the brains were placed in Fomblin solution (Ausimont, Thorofare, NJ) and imaged on a 4.7 T Bruker Biospec MR system.

Scanning Parameters

The pulse sequence used for diffusion acquisition was a 3D diffusion-weighted spin-echo echoplanar imaging sequence, time repetition/time echo 1000/40 ms, with an imaging matrix of 128 × 128 × 128 pixels. Sixty diffusion-weighted measurements and one non diffusion-weighted measurement were acquired, corresponding to a cubic lattice in Q-space at b = 8000 s/mm^2 with small delta = 12.0 ms, large delta = 24.2 ms. The total acquisition time was approximately 2 h for each imaging session. Spatial resolution was 415 × 500 × 550 μm for W17–22, 525 × 525 × 600 μm for W31, and 700 × 830 × 860 μm for W38 and W40. Brains of W17 were imaged as whole brains, but due to bore size, other ages were imaged one hemisphere at a time.

Diffusion Data Analyses—Tractography

We used a streamline algorithm for diffusion tractography (Mori et al. 1999) as in previous publications (Takahashi et al. 2010, 2011) to highlight whole-brain fiber trajectories and their transition into mature forms. It should be noted that tractography helps us visualize patterns of tissue coherence over the brain. Trajectories were propagated by consistently pursuing the orientation vector of least curvature. We terminated tracking when the angle between 2 consecutive orientation vectors was greater than the given threshold (40°), or when the fibers extended outside of the brain surface, by using mask images of the brains created by MRIcro (http://www.sph.sc.edu/comd/rorden/mricro.html) for each specimen. We use a brain mask to terminate tracts as we explore the coherence in the brain and not in the fluid we submerse the brain in, i.e., we mask to extract the connectivity in the brain. End points are therefore constrained to be within brain tissue. As in previous studies, no fractional anisotropy (FA) threshold was applied (Vishwas et al. 2010; Takahashi 2010). In many tractography studies, FA values are used to terminate fibers in the gray matter, which in adults has lower FA values than the white matter. However, as one of the objectives of our study was to detect fibers in low FA areas, we used brain mask volumes to terminate tractography fibers instead of the FA threshold. This method has been used previously (Takahashi et al. 2011) and is an acceptable alternate method (Schmahmann et al. 2007; Wedeen et al. 2008). Diffusion Toolkit and TrackVis (http://trackvis.org) were used to reconstruct and visualize tractography pathways. The color-coding of tractography pathways is based on a standard RGB code, applied to the vector between the endpoints of each fiber.

Results

We report our findings as pathways for conceptual purposes only, with the understanding that "pathways" represent coherent tissue structure. We use the term "radial coherence" or "radial structure" as pathways running across the cerebral mantle or a part of cerebral mantle perpendicular to the brain surface. Radial coherent structure could arise from radial glial fibers and streams of migrating neurons, as well as from efferent and afferent axons (Takahashi et al. 2011). We present the evolution of fiber pathways as main results and the relationships between fibers and gyral structures as preliminary findings to be fully studied with histologic correlations in the future.

Tractography at W17—Dominant Radial Pathways with Immature Forms of Projection, Limbic and Few Emergent Association Pathways

Predominant coherent radial pathways from the ventricular margin to the brain surface were found in most brain areas (Fig. 2*A*), coursing throughout the cortical pate (CP), subplate (SP), intermediate zone (IZ), and ventricular zone (VZ) (Fig. 3*A* coronal images). These radial structures tended to be longer in dorsal frontal and parietal areas (e.g., areas labeled (a) in

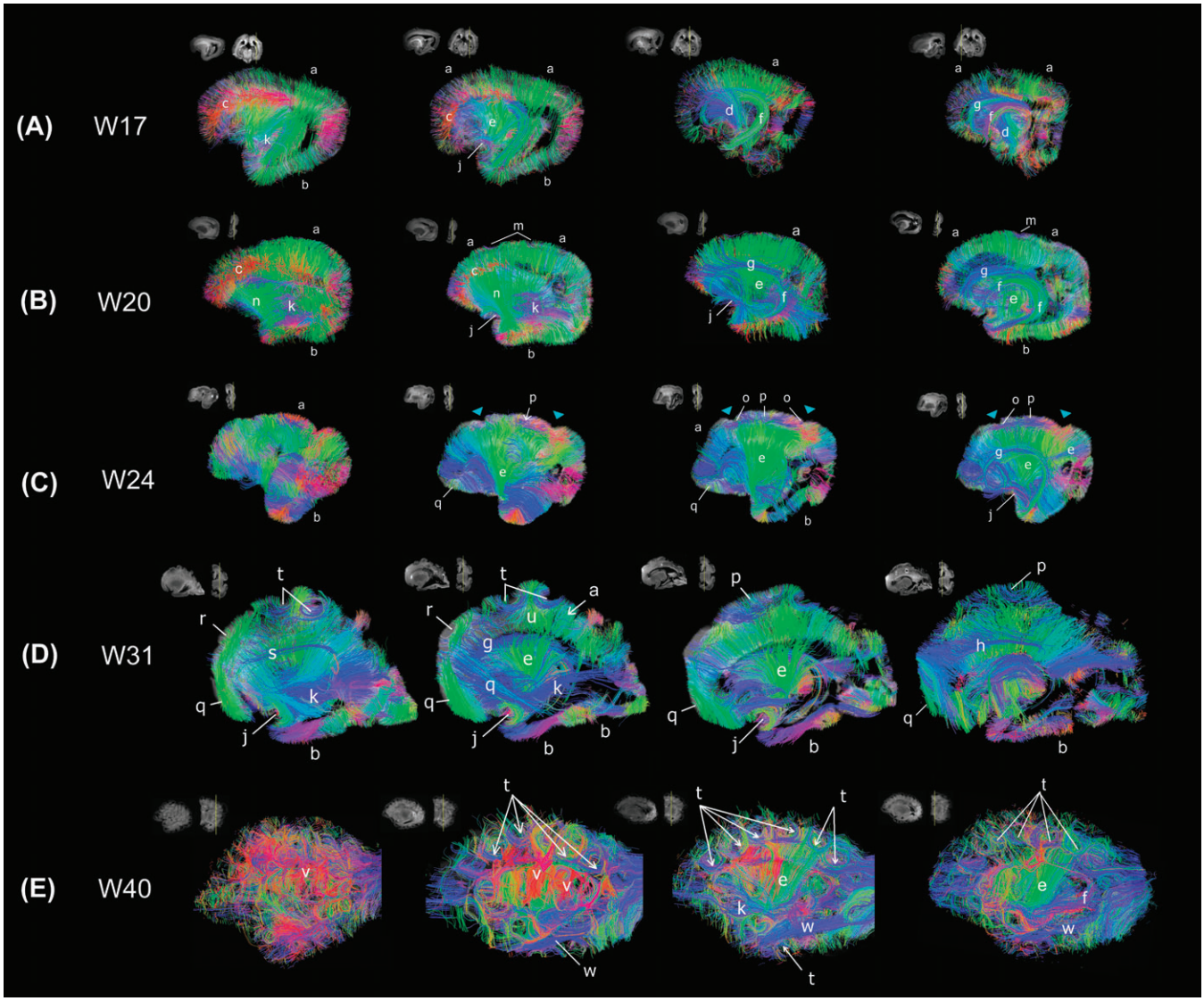

Figure 2. Tractography pathways at W17 (A), W20 (B), W24 (C), W31 (D), and W40 (E). (*A*) Tractography at W17—dominant radial pathways with immature forms of projection, limbic, and few emergent association pathways. a: radial pathways (in dorsal areas), b: radial pathways (in ventral areas), c: radial pathways (medio-lateral horizontal direction), d: corticospinal tract, e: corticothalamic/thalamocortical tract, f: fornix, g: ganglionic eminence, j: uncinate fasciculus, k: inferior fronto-occipital fasciculus. We put the label (k) deep inside from the temporal lobe where the tract is running, which in the sagittal view looks running through the temporal lobe, but the tract is actually running between the frontal and occipital cortices. (*B*) Tractography at W20—dominant radial pathways and emerging long-range connectivity patterns. a: radial pathways (in dorsal areas), b: radial pathways (in ventral areas), c: radial pathways (medio-lateral horizontal direction), e: corticothalamic/thalamocortical tract, f: fornix, g: ganglionic eminence, j: uncinate fasciculus, k: inferior fronto-occipital fasciculus, m: superficial horizontal pathways, n: frontotemporal pathways. Similar features were noted in W22 specimen (not shown). (*C*) Tractography at W24—less predominant radial pathways in dorsal frontal, parietal and inferior frontal lobes, and emergent short-range corticocortical and long-range association pathways. a: radial pathways (in dorsal areas), b: radial pathways (in ventral areas), e: corticothalamic/thalamocortical tract, f: fornix, g: ganglionic eminence, j: uncinate fasciculus, o: corticocortical pathways (in parietal and parieto-fontal areas), p: corticocortical pathways (in parietal areas without gyrus), q: corticocortical pathways (in ventral frontal areas). (*D*) Tractography at W31—less dominant radial pathways in the temporal and occipital lobes, emergent short-range corticocortical and long-range association pathways ventrally. a: radial pathways (in dorsal areas), b: radial pathways (in ventral areas), e: corticothalamic/thalamocortical tract, f: fornix, g: ganglionic eminence, h: cingulum, j: uncinate fasciculus, k: inferior fronto-occipital fasciculus, p: corticocortical pathways (in parietal areas without gyrus), q: corticocortical pathways (in ventral frontal areas), r: corticocortical pathways (in superior frontal areas), s: superior fronto-occipital fasciculus, t: cortical u-fibers, u: radial pathways between gyral apices and ventricular regions. (*E*) Tractography at W40—no evident radial pathways, abundant complex, crossing short- and long-range corticocortical association pathways. e: corticothalamic/thalamocortical tract, f: fornix, k: inferior fronto-occipital fasciculus, t: cortical u-fibers, v: corticocortical pathways (between the insula and temporal cortex), w: inferior longitudinal fasciculus. Similar features were noted in W38 specimen (not shown). In all panels, we show tractography pathways that pass through a sagittal slice that is shown as an insert in upper left corner. In a coronal slice next to the sagittal slice, the location of the sagittal slice is shown as a yellow line. For visualization purposes in the figures, we restricted the percentages of the number of detected tractography pathways in the following ways. We showed only 70% of the tractography fibers that touched each sagittal slice and were more than 2 mm in length. The label g actually points at tangential pathways in the ganglionic eminence structure running in the anterior–posterior direction (shown in blue). Colors indicate spatial relationships between fiber end points. Red: left–right, blue: anterior–posterior, and green: dorsal–ventral orientation. As we explain in the text, callosal connections in the specimens were disrupted at the midline at autopsy, so callosal tractography pathways appeared in green (dorsoventral direction: from the corpus callosum to the cortex).

Fig. 2*A*) than in ventral frontal, temporal, and occipital areas (e.g., areas labeled (b) in Fig. 2*A*). This reflected differences in the thickness of the cerebral mantle in these locations. Radial pathways in the dorsal frontal areas running in the mediolateral horizontal direction (labeled red (c) in Fig. 2*A*) were abundant at this stage.

Projection pathways such as the corticospinal tracts (marked (d) in Fig. 2*A*; in blue) and corticothalamic/thalamocortical

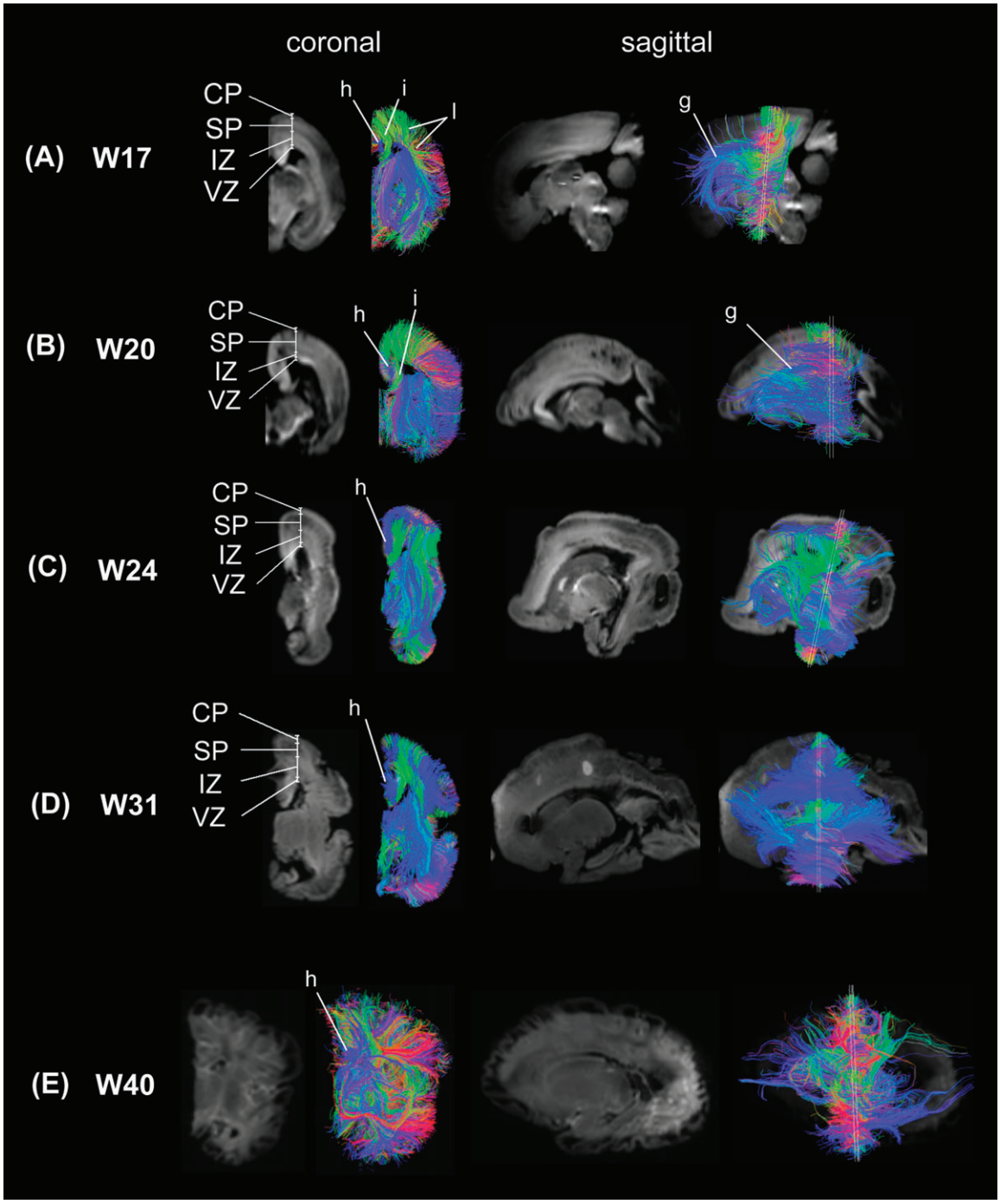

Figure 3. Coronal, sagittal, and oblique images of mean diffusion images and superimposed tractography pathways at (*A*) W17, (*B*) W20, (*C*) W24, (*D*) W31, and (*E*) W40. CP: cortical plate, SP: subplate, IZ: intermediate zone, VZ: ventricular zone. g: ganglionic eminence, h: cingulum, i: callosal pathway, l: corticocortical pathways (parietotemporal).

fibers (marked (e) in Fig. 2*A*; in green) were clearly delineated. Some limbic structures, for instance, the fornix (marked (f) in Fig. 2*A*; in purple and green), were clearly observed at this stage, whereas the cingulum bundle was small and not completely resolved (marked (h) in Fig. 3*A*; in blue). We also noted another pathway, separate from the fornix, running along the ventricular margin (marked (g) in Figs 2*A* and 3*A*; in blue) that corresponded to the lateral ganglionic eminence. Thus, the ganglionic eminence showed a strongly tangential organization (Fig. 4*A–C*). Pathways branching from the ganglionic eminence were running throughout CP, SP, IZ, and VZ (Fig. 3*A* sagittal images).

Callosal pathways (marked (i) in Fig. 3*A*; in green) appeared to terminate prior to reaching the midline, but this finding reflected the artifactual division of the corpus callosum during brain removal. Similarly, the anterior commissure was artifactually divided in the midline.

Interestingly, within-lobes, short-range corticocortical pathways were found only in specific areas of the parietal and occipital lobes (Fig. 3*A* (l)) and not in the temporal and frontal

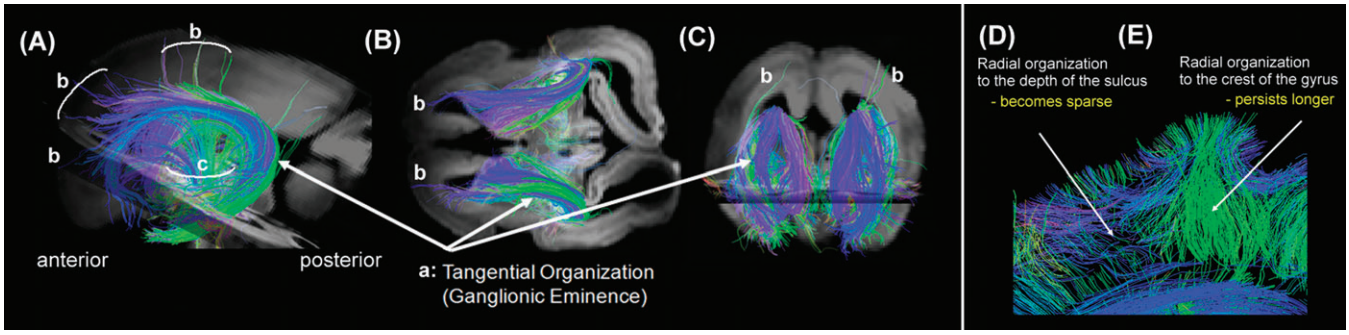

Figure 4. (*A*) Sagittal, (*B*) axial, and (*C*) coronal views of tangential pathways associated with the ganglionic eminence at W17 (a). (b) Pathways continuous from the tangential pathways to the cerebral mantle and (c) thalamocortical and corticospinal tracts. These pathways were identified by using an axial slice shown in (*A*) as a slice filter. (*D*, *E*) A magnified image around Figure 2*D* (t) and (u). (*D*) Radial organization to the crests of the gyri and (*E*) radial organization to the depths of the sulci.

lobes. These pathways were oriented in the dorsal–ventral direction on coronal slices. The emerging short-range cortico-cortical pathways were observed through the subplate and intermediate zone (Fig. 3*A* coronal images).

We observed a frontotemporal pathway running between the inferior frontal lobe and the anterior temporal pole (probably the uncinate fasciculus, marked (j) in Fig. 2*A*, in purple) as well as a cluster of fronto-occipital pathways projecting from the inferior frontal lobe to the posterior areas in the brain (probably the inferior fronto-occipital fasciculus, marked (k) in Fig. 2*A*; in grayish blue). The other cortico-cortical pathways were found only in a restricted dorsal brain area (marked (l) in Fig. 3*A*, in green). These between-lobe pathways were oriented in the anterior–posterior direction on sagittal slices.

Overall, brain structure at this stage can be characterized by a strong radial coherence with minimal regional variation. Only a few long-range association pathways were visible. The minimal regional variation resulted from the coherent structures that had the expected shape and location of the limbic and emergent corticocortical association pathways connecting specific brain areas: between dorsal and ventral parietal areas, between dorsal and ventral occipital areas, and between ventral frontal and anterior temporal areas.

Tractography at W20 and W22—Dominant Radial Pathways and Emerging Long-Range Connectivity

Radial coherence remains dominant at W20 and W22 with regional variation in length due to differences in thickness of the cerebral mantle (Fig. 2*B* (a, b)). Radial pathways identified in the dorsal frontal areas (Fig. 2*B* (c), red pathways) were reduced compared with those at W17, suggesting a decrease in the radial coherence. In addition, the radial tractography pathways remained continuous from the ventricular margin to the brain surface, across the CP, SP, IZ (Fig. 3*B*, coronal images). Pathways branching from the ganglionic eminence were less prominent at this stage (Fig. 3*B*, sagittal images).

Projection pathways such as the corticospinal tracts (marked (d) in Fig. 2*B*) and corticothalamic/thalamocortical fibers (marked (e) in Fig. 2) were clearly delineated. Fornix (Fig. 2*B* (f), in green) and the lateral ganglionic eminence pathways (Fig. 2*B* (g), in blue) were observed, as in W17. Intrahemispheric association pathways became more prominent at this age compared with W17. The uncinate fasciculus (Fig. 2*B* (j), in green) became thicker and increased in coherence. Superficial horizontal pathways were observed in dorsal brain areas (Fig. 2*B* (m)). In addition, the frontotemporal pathways became more prominent (Fig. 2*B* (n), in green). The inferior fronto-occipital fasciculus (Fig. 2*B* (k), in blue) also became more prominent and longer compared with that at W17.

Overall, the basic structure at W20 was comparable to that at W17, but there were newly identified corticocortical pathways as well as existing corticocortical pathways with increased coherence suggesting increasing corticocortical connectivity. In addition, the density of radial pathways was reduced compared with W17, suggesting a regression of radial coherence. Similarly, brain structure at W22 remained similar to that at W20. However, at W22, we observed parasagittal corticocortical fiber pathways running horizontally (medio-laterally) throughout the dorsal forebrain from anterior to posterior (Fig. 5 upper panel (A), red and orange). These pathways were found specifically at W22 and were distinct from callosal connections (Fig. 5 upper panel (B)). These pathways appeared to be dense intralobular frontal cortico-cortical association fibers. Accompanying these increases in corticocortical pathways, and perhaps because of them, radial pathways became less coherent than at earlier stages, especially in the dorsal brain regions.

Tractography at W24—Less Predominant Radial Pathways in Dorsal Frontal, Parietal and Inferior Frontal Lobes, and Emergent Short-Range Corticocortical and Long-Range Association Pathways

Long-range radial coherence in the dorsal brain regions persisted at this stage (Fig. 2*C* (a), although less prominent in several brain regions. Radial tractography pathways in dorsal brain areas became less coherent, while in ventral areas coherent radial tractography pathways were still observed (Fig. 3*C* coronal images). Interestingly, radial pathways seen running in a dorsal medio-lateral direction in earlier stages (Fig. 2*A* (c) and Fig. 2*B* (c), red pathways) were not observed at W24; instead we saw emergent corticocortical pathways in an anterior–posterior direction (Fig. 2*C* (o) and (p)). Projection pathways and corticothalamic/thalamocortical fibers (marked (e) in Fig. 2*C*) were clearly delineated.

In dorsal brain areas, multiple types of emerging short corticocortical pathways were observed in IZ (Fig. 2*C* (o)

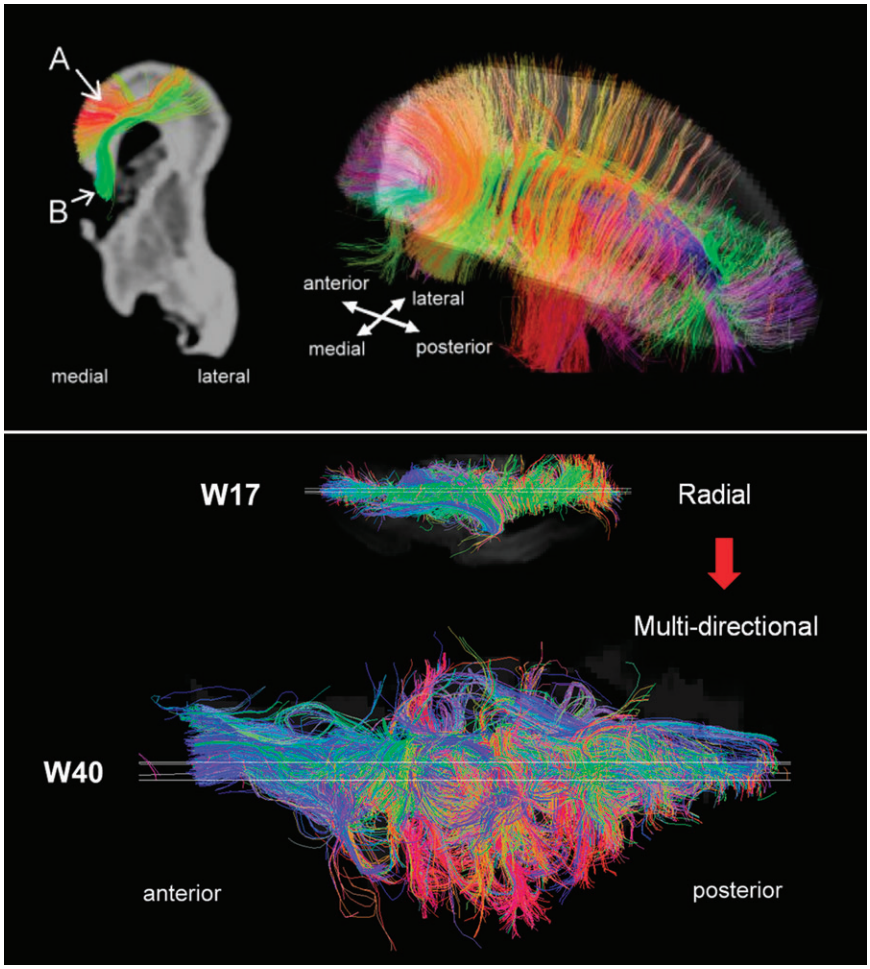

Figure 5. Upper panel: Tractography pathways at W22. Colors indicate spatial relationships between fiber end points. Red: left–right, blue: anterior–posterior, and green: dorsal–ventral orientation. As we explain in greater detail in the text, callosal connections in the specimens were disconnected at the midline during craniotomy, so callosal tractography pathways appeared in green (dorsoventral direction: from the corpus callosum to the cortex). (*A*) Corticocortical pathways (in dorsal areas including occipital, parietal, and frontal areas). (*B*) Callosal pathways. We selected only 2 types of pathways of interest using appropriate slice filters. Lower panel: axial views of fiber pathways at W17 and at W40. Only fibers that pass a sagittal plane (shown as a white slice in the Figure) are shown.

and (p), in blue, and Fig. 3*C*, coronal and sagittal images). Furthermore, in a small anterior region of the inferior frontal lobe, we also observed that short corticocortical pathways were beginning to emerge (Fig. 2*C* (q), in blue/green). Other areas in the frontal lobe, as well as the temporal and occipital lobes, still contain predominantly radial coherence as in earlier stages.

Gyrification has begun with formation of the parieto-occipital sulcus (Fig. 2*C*, right blue arrow) and the central sulcus (Fig. 2*C*, left blue arrow) above the horizontal pathways (Fig. 2*C* (c), blue pathways). However, relationships between the gyral formation and corticocortical fiber pathways are not clear at this stage. These 2 sulci in the dorsal area were close to the horizontal pathways forming the corticocortical pathways, but those pathways connected broad areas around the sulcus (Fig. 2*C* (o)) as well as areas surrounding the sulci (Fig. 2*C* (p), in blue). In the inferior frontal region, there was no gyrification superficial to the short corticocortical pathways.

In summary, brain connectivity at this stage is characterized by emergent short-range corticocortical fiber pathways in dorsal brain areas and in a restricted area of the inferior frontal lobe. Radial coherence becomes less prominent in brain regions with extensive corticocortical connectivity.

Tractography at W31—Less Dominant Radial Pathways in the Temporal and Occipital Lobes, Emergent Short-Range Corticocortical and Long-Range Association Pathways Ventrally

At W31, radial pathways in the frontal and parietal lobes are further reduced in number but still are regionally present (Fig. 2*D* (a)). Radial pathways also become less predominant in the temporal and occipital lobes (Fig. 2*D* (b)), with the emergence of the short-range corticocortical pathways. Radial pathways in ventral areas were still observed (Fig. 3*D* coronal images).

In dorsal brain areas, multiple types of emerging white matter pathways were observed in IZ as at W24 (Fig. 3*D*, coronal and sagittal images). The dorsal part of the cingulum bundle is also detected at this stage, but its posterior limb down to the medial temporal lobe is not yet visible (Fig. 2*D* (h), in blue). Callosal pathways are clearly imaged (Fig. 2*D* (i), in green), as they emerge from the midline and curve upward toward the cortical plate. The ganglionic eminence (Fig. 2*D* (g),

blue pathways) was still observed. Projection pathways and corticothalamic/thalamocortical fibers (marked (e) in Fig. 2*D*) were clearly delineated.

Short-range U-shaped corticocortical pathways in dorsal brain regions curve along with emergent gyral structures (Fig. 2*D* (t), in blue) and are associated with increased folding the cortex between the central and parieto-occipital sulci. We also noted radial fibers running down to the ventricular margin from the crest of the gyri (Fig. 2*D* (u), in green) and corticocortical pathways without a gyrus (Fig. 2*D* (p), in blue). Figure 4*D*,*E* shows a magnified image in the same region as Figure 2*D* (t) and (u). The radial organization tended to persist longer in crests of the gyri (Fig. 4*D*) than at depths of the sulci (Fig. 4*E*). Short-range intra-frontal pathways were first observed at 24W in a small region of the inferior frontal lobe, but by W31, they have increased in both number and length and are clearly imaged (Fig. 2*D* (q), in green). In addition to the intra-frontal pathways in the inferior frontal lobe, another group of intra-frontal pathways becomes visible in the superior frontal lobe (Fig. 2*D* (r), in green). These 2 intra-frontal pathways are located adjacent to one another, connecting the superior and middle frontal gyri and the middle and inferior frontal gyri but do not appear to be continuous with each other. The long-range inferior fronto-occipital fasciculus that was imaged at earlier stages in an immature, shorter form, is imaged clearly and in its full length at this stage (Fig. 2*D* (k), in blue). The superior fronto-occipital fasciculus, which was not detected earlier, is also clearly imaged at this stage (Fig. 2*D* (s), in blue).

In summary, connectivity at this stage is characterized by emergent short-range corticocortical fibers throughout the whole brain with clearly visible long-range association pathways and regression of radial organization with an overall dorsal ventral gradient. Developing gyri were associated with emerging subcortical U-fibers at the depth of the sulci and persistent radial pathways extending to the crest of the gyri.

Tractography at W38 and W40—No Evident Radial Pathways, Abundant Complex, Crossing Short- and Long-Range Corticocortical Association Pathways

At W38 and W40, no radial pathways were confidently identified (Fig. 3*E*). Even in the right lower panel in Figure 2*E*, in which we restricted visualization of fiber pathways to those starting or ending in the sagittal slice, we did not observe a clear radial structure. Projection pathways and corticothalamic/thalamocortical fibers (marked (e) in Fig. 2*E*) were clearly delineated. The ganglionic eminence was not confidently detected at this stage. Instead, we detected many U-fibers in full length along gyral structures (Fig. 2*E* (t), in blue). Figure 2*E* ((v), in red) also shows short-range corticocortical pathways between the insula (medial) and the temporal lobe (lateral). In addition to the inferior fronto-occipital fasciculus (Fig. 2*E* (k), in blue), which was also imaged at W31, the inferior longitudinal fasciculus (Fig. 2*E* (w), in blue) was clearly detected in this stage.

In summary, connectivity at this stage is characterized by an adult-like corticocortical pattern of fiber pathways involving the whole brain and the absence of immature radial coherence and tangential organization associated with the ganglionic eminence. In other words, the initially observed highly radial coherence at W17 had regressed and given rise to multidirectional corticocortical connectivity at W40 (Fig. 5, lower panel).

Discussion

From W17 to 40 of fetal human brain development, we observed regression of the initial radial organization of the cerebral mantle and tangential organization of the ganglionic eminence. As these structures regressed, intracerebral connectivity emerged in a sequential manner, starting from dorsal posterior brain areas, continuing in an anteroventral direction, and ending in inferior temporal and inferior frontal lobes. This observed order of regional radial and tangential regression with emergence of intracerebral connectivity follows the same order of normal gyrification (White et al. 2010). In addition, we noted that the radial pathways to the crests of the gyri appears to regress later than those to the depths of the sulci and horizontal fiber pathways tended to emerge before gyri and sulci.

Development of Brain Connectivity, as Suggested by Tractography Results—Decreasing Radial Appearance and Emerging Expansion of Corticocortical Pathways

In W17 and W20 brains, we observed a dominant radial organization throughout the cerebral mantle. Histiolgically at this stage of development, large numbers of neurons migrate along radial glia stretched between the ventricular germinal zone and the pial edge of the CP. Upon arrival, these young neurons arrange themselves in an inside-out pattern, so that the later arrivals climb over the earlier ones and come to rest closer to the pial surface (Sidman and Rakic 1973). The observed radial organization is likely the result of a mixture of radial glial fibers, migrating neurons and glial cells (glial migration streams), which cannot be differentiated by current diffusion imaging techniques. A single migratory column is below the resolution of imaging, but groups of columns could be imaged as one tractography pathway. The radial organization we detected regressed during the time assessed, probably as a result of the transformation of radial glia to astrocytes and the termination of neuronal migration. Although radial vascular structures could also be a contributing factor to the radial coherence of the cerebral mantle, the regression of the radial coherence when radial vascular structure is still prominent suggest that this is unlikely. The regional variation in the timing of the radial regression in our study may help explain the different times reported for the termination of neuronal migration in the literature (McKinstry et al. 2002; Huang et al. 2009; for review, Campbell and Götz 2002).

Pathways that were presumed thalamocortical/corticothalamic tracts were evident at W17 but became more evident at later gestational ages. Although thalamocortical afferent fibers have been reported to reach just below the cortical plate at around W20–23 (Kostovic and Jovanov-Milosevic 2006), immature axonal fibers must be present in deeper subcortex prior to W20–23 (Kostovic and Rakic 1984), which is consistent with our current study. Tissue coherence suggesting presence of corticocortical pathways has also been reported in previous DTI studies of fetal brain specimens earlier than W20 (e.g., Huang et al. 2009). Thus, findings by us and others correspond to the tissue expression of immature axonal markers in the human parietal white matter at W20–23 (Haynes et al. 2005). Corticocortical association fibers have been found in the cortical plate around W23–25 (Kostovic and Jovanov-Milosevic 2006), but immature axons of association fibers have been imaged as early as W15 (Vasung et al. 2010),

which is consistent with our findings. Decreases in ipsilateral corticocortical connections observed after 22W may be due to axonal loss from failure of final targeting or from pruning after initial exuberant over-connectivity (Innocenti and Price 2005).

Honig and colleagues studied vimentin immunoreactivity—a marker for neuroepithelial and radial glial cells—in the developing visual cortex at weeks 14, 19, 36 (preterm), and 79 (postterm) (Stagaad and Mollgard 1989; Wilkinson et al 1990; Sarnat 1992; Honig et al. 1996) and found that in the visual cortex, vimentin immunoreactivity decreased dramatically after W36, accompanied by the loss of radial structure (Honig et al. 1996). However, there was a wide sampling gap in their study between weeks 19 and 36, making it likely that less dramatic losses in radial architecture occur earlier than W36, which would be consistent with our present findings. However, the process is further complicated by the fact that as glial processes increasingly disappear, subcortical corticocortical axons grow radially into the cortical plate, followed by corticocortical axons, which would increase the radial architecture but only in the subcortical and cortical regions (Takahashi et al. 2011). Thus, the picture that emerges is likely the result of all these steps proceeding in order during development with the net effect of decreasing the radial appearance and increasing the corticocortical connections (Kostovic and Jovanov-Milosevic 2006; Kostovic and Judas 2010) with the decrease in some pathways possibly representing pruning of exuberant connectivity known to begin in the late third trimester (for discussion, Billiards et al. 2006).

Tangential Organization of the Ganglionic Eminence

The ganglionic eminence constitutes tightly packed cells along the ventricular margin above the thalami and the caudate nucleus and disappears by the end of mid-gestational weeks (W30–35) (Rados et al. 2006). The structure and directions of pathways in the ganglionic eminence were described by Huang et al. (Huang et al. 2006, 2009) and Vasung et al. (2011). The course and location of the tract labeled by (g) in Figure 3*A,B* in the current study correspond to the ganglionic eminence in the paper of Vasung et al. (2011) and Huang et al. (2009), and are distinct from the periventricular pathways shown in Vasung et al. (2011). The tangential pathways associated with the lateral ganglionic eminence gradually disappear from W17 through W40 in our current study, which is consistent with the disappearance of the migration streams and elongated glial processes in the human brain as they move tangentially in the ganglionic eminence before migrating to the cortex or thalamus (e.g., Letinic et al. 2002 and Nadarajah et al. 2003).

Is Development of Connectivity Related to Gyral Formation?

We showed some preliminary results on the relationships between fiber and gyral development. It is well established, with few exceptions, that gyrification starts in the dorsal parieto-occipital areas and proceeds anteroventrally to involve first superior frontal and superior temporal region and then inferior frontal and inferior temporal cortex (Chi et al. 1977; Welker 1990; Armstrong et al. 1995; Zilles et al. 1997; Blanton et al. 2001; Dubois et al. 2008; for review, White et al. 2010 A number of hypotheses have been proposed on the mechanisms that underlie normal gyrification in the fetal brain, such as differential growth rates in different brain regions, which cause tension and local tissue deformation (His 1874), differential growth between gyri and sulci (Retzius 1891, Barron 1950), cytoarchitectonic differentiation leading to thinner and thicker adjacent cortices, which causes buckling (Connolly 1950), and differential expansion of the individual cortical layers (Richman et al. 1975; Welker 1990; Van Essen 1997; Toro and Burnod 2005; Hilgetag and Barbas 2005, 2006). However, these theories of cortical folding need to explain why convolutions are modified in relation to the underlying cortical connectivity (Goldman-Rakic 1980; Goldman-Rakic and Rakic 1984). Another theory emerged postulating that viscoelastic tension exerted by cortical fibers contributes to the shaping of cortical convolutions (Goldman-Rakic and Rakic 1984; Van Essen 1997; Hilgetag and Barbas 2005).

Our tractography results suggest that gyrification of the cortex has a specific relationship to underlying patterns of connectivity. In addition, the relative persistence of radial organization under the gyral crests suggests that there might be a relationship between gyral folding and a longer period of migration to the gyral crests. This process occurs topographically from dorsal-posterior brain regions toward ventral-anterior ones, in the evolution of connection patterns and in the subsequent regional regression of radial organization and gyrification of the cortex. Although these observations cannot by themselves establish causality between the emergence of connections and the subsequent regional regression of radial structure and development of gyri and sulci, their intimate chronological relationship suggests that developing connectivity as well as regional variations in duration of migration may both play a role in gyrification. Proof of the causal relationship between fiber pathways, duration of migration, and gyral formation will need to wait for models where independent manipulation of axonal connections and radial migration can be performed.

Advantages and Limitations of the Current Study and Future Potential

Unlike histology, MRI does not provide direct evidence of the existence of fiber pathways or specific neural components such as axons, glial fibers, or aligned cellular components. This limitation is part of the nature of present day MRI studies, and histology is still clearly superior to MRI in terms of resolution and specificity. However, one great advance of MRI over histology is its ability to provide a whole-brain 3D visualization that allows for easy interpretation of changes in one region in relation to changes in another. Nevertheless, the detailed correlation between histology and imaging is still the gold standard that permits not only a fuller picture but also the better understanding of the limitations of each method alone.

Our measures are volume averages over 400–800 cubic microns and therefore we cannot tell whether the radial fibers disappear, or instead are obscured by a more abundant tangential organization. However, we feel that this global view on regional dominance is important as we do detect regional variability that has not been appreciated previously. Therefore, we hope this work will inspire further immunohistochemical validation that otherwise would not occur.

Finally, it has long been recognized that disorders of brain morphology associated with grossly abnormal gyral folding such as polymicrogyria and pachygyria are associated with the

development of abnormal cognitive function and with epilepsy (Barkovich et al. 1995; Jansen et al. 2005). Recently, there has been growing awareness of the fact that more subtle developmental disturbances of gyral folding can also lead to developmental, albeit milder neurological disorders such as dyslexia (Galaburda et al. 1985), schizophrenia (Noga et al. 1996; White et al. 2003; Narr et al. 2004), autism (Levitt et al. 2003), William's syndrome (Galaburda et al. 2003; Van Essen et al. 2006), and Rett syndrome (Joyner et al. 2009), and a number of studies have shown subtle abnormal white matter development in such disorders suggesting altered connectivity (Nowell et al. 1988; Rapoport et al. 2001). It is therefore essential to develop a clear picture of the normal patterns and timing of development of brain pathways and to interpret the role of white matter pathways (e.g., Takahashi et al. 2007, 2008) in order to more accurately diagnose subtle disorders of brain connectivity during development. At this point, the ability to apply our methods to the in vivo fetal population is limited by fetal motion and size, however, progress is being made, in that major pathways are beginning to be identified (Kasprian et al. 2008). Collaborations are underway to attempt to meet these challenges because tractography has a strong potential to increase our understanding of normal and abnormal fetal brain development in utero.

Funding

Ellison Medical Foundation (#208556); NICHD grant (PO1 HD057853) to A.M.G; and Children's Hospital Boston.

Notes

We appreciate George Dai and Joseph Mandeville for their technical support. We thank Nichole Eusemann for editorial comments. *Conflict of Interest* : None declared.

References

Armstrong E, Schleicher A, Omran H, Curtis M, Silles K. 1995. The ontogeny of human gyrification. Cereb Cortex. 5:56–63.

Barbas H, Rempel-Clower N. 1997. Cortical structure predicts the pattern of corticocortical connections. Cereb Cortex. 7:635–646.

Barkovich AJ, Rowley H, Bollen A. 1995. Correlation of prenatal events with the development of polymicrogyria. Am J Neuroradiol. 16: 822–827.

Barron DH. 1950. An experimental analysis of some factors involved in the development of the fissure pattern of the cerebral cortex. J Exp Zool. 113:553–581.

Billiards SS, Pierson CR, Haynes RL, Folkerth RD, Kinney HC. 2006. Is the late preterm infant more vulnerable to gray matter injury than the term infant? Clin Perinatol. 33:915–933. Available from: http://www.ncbi.nlm.nih.gov.ezp-prod1.hul.harvard.edu/pubmed/17148012.

Blanton RE, Levitt JG, Thompson PM, Narr KL, Capetillo-Cunliffe L, Nobel A, Singerman JD, McCracken JT, Toga AW, et al. 2001. Mapping cortical asymmetry and complexity patterns in normal children. Psychiatry Res. 107:29–43.

Burkhalter A, Bernardo KL, Charles VJ. 1993. Development of local circuits in human visual cortex. J Neurosci. 13:1916–1931.

Campbell K, Götz M. 2002. Radial glia: multi-purpose cells for vertebrate brain development. Trends Neurosci. 25:235–238.

Caviness VS, Kennedy DN, Bates J, Makris N. 1996. The developmental neuroimaging: mapping the development of brain and behaviour. New York: Academic Press. p. 3–14.

Chi JG, Dooling EC, Gilles FH. 1977. Gyral development of the human brain. Ann Neurol. 1:86–93.

Connolly C. 1950. External morphology of the primate brain. Springfield (IL): Charles C Thomas.

Dubois J, Benders M, Borradori-Tolsa C, Cachia A, Lazeyras F, Ha-Vinh Leuchter R, Sizonenko SV, Warfield SK, Mangin JF, Hüppi PS. 2008. Primary cortical folding in the human newborn: an early marker of later functional development. Brain. 131:2028–2041.

Encha-Razavi F, Sonigo P. 2003. Features of the developing brain. Childs Nerv Syst. 19:426–428.

Galaburda AM, Sherman GF, Rosen GD, Aboitiz F, Geschwind N. 1985. Developmental dyslexia: four consecutive patients with cortical anomalies. Ann Neurol. 18:222–233.

Galaburda AM, Holinger D, Mills D, Reiss A, Korenberg JR, Bellugi U. 2003. Williams syndrome. A summary of cognitive, electrophysiological, anatomofunctional, microanatomical and genetic findings. Rev Neurol. 36(Suppl 1):S132–S137.

Goldman-Rakic PS. 1980. Morphological consequences of prenatal injury to the primate brain. Prog Brain Res. 53:1–19.

Goldman-Rakic PS, Rakic P. 1984. Experimental modification of gyral patterns. In: Geschwind N, Galaburda A, editors. Cerebral dominance. Cambridge (MA): Harvard University Press. p. 179–192.

Haynes RL, Borenstein NS, Desilva TM, Folkerth RD, Liu LG, Volpe JJ, Kinney HC. 2005. Axonal development in the cerebral white matter of the human fetus and infant. J Comp Neurol. 484:156–167.

Hevner RF. 2000. Development of connections in the human visual system during fetal mid-gestation: a DiI-tracing study. J Neuropathol Exp Neurol. 59:385–392.

Hilgetag CC, Barbas H. 2005. Developmental mechanics of the primate cerebral cortex. Anat Embryol. 210:411–417.

Hilgetag CC, Barbas H. 2006. Role of mechanical factors in the morphology of the primate cerebral cortex. PLoS Comput Biol. 2(3):e22.

His W. 1874. Unsere Korperform und das physiologische Problem ihrer Entstehung. Leipzig (Germany): F.C.W. Vogel.

Honig LS, Herrmann K, Shatz CJ. 1996. Developmental changes revealed by immunohistochemical markers in human cerebral cortex. Cereb Cortex. 6:794–806.

Huang H, Zhang J, Wakana S, Zhang W, Ren T, Richards LJ, Yarowsky P, Donohue P, Graham E, van Zijl PC, et al. 2006. White and gray matter development in human fetal, newborn and pediatric brains. Neuroimage. 33:27–38.

Huang H, Xue R, Zhang J, Ren T, Richards LJ, Yarowsky P, Miller MI, Mori S. 2009. Anatomical characterization of human fetal brain development with diffusion tensor magnetic resonance imaging. J Neurosci. 29:4263–4273.

Innocenti GM, Price DJ. 2005. Exuberence in the development of cortical networks. Nat Rev. 6:955–965.

Jansen AC, Leonard G, Bastos AC, Esposito-Festen JE, Tampieri D, Watkins K, Andermann F, Andermann E. 2005. Cognitive functioning in bilateral perisylvian polymicrogyria (BPP): clinical and radiological correlations. Epilepsy Behav. 6:393–404.

Joyner AH, Rddey CJ, Bloss CS, Bakken TE, Rimol LM, Melle I, Agartz I, Djurovic S, Topol EJ, Schork NJ, et al. 2009. A common MECP2 haplotype associates with reduced cortical surface area in humans in two independent populations. Proc Natl Acad Sci U S A. 106: 15483–15488.

Kasprian G, Brugger PC, Weber M, Krssák M, Krampl E, Herold C, Prayer D. 2008. In utero tractography of fetal white matter development. Neuroimage. 43:213–224.

Kostovic I, Jovanov-Milosevic N. 2006. The development of cerebral connections during the first 20-45 weeks'gestation. Semin Fetal Neonat Med. 11:415–422.

Kostovic I, Judas M. 2010. The development of the subplate and thalamo-cortical connections in the human foetal brain. Acta Paediatr. doi: 10.1111/j.1651–2227.2010.01811.x.

Kostovic I, Rakic P. 1984. Development of prestriate visual projections in the monkey and human fetal cerebrum revealed by transient cholinesterase staining. J Neurosci. 4:25–42.

Kostovic I, Rakic P. 1990. Developmental history of the transient subplate zone in the visual and somatosensory cortex of the macaque monkey and human brain. J Comp Neurol. 297:441–470.

Leergaard TB, White NS, de Crespigny A, Bolstad I, D'Arceuil H, Bjaalie JG, Dale AM. 2010. Quantitative histological validation of

diffusion MRI fiber orientation distributions in the rat brain. PLoS One. 5:e8595.
Letinic K, Zoncu R, Rakic P. 2002. Origin of GABAergic neurons in the human neocortex. Nature. 417:645–649.
Levitt JG, Blanton RE, Smalley S, Thompson PM, Guthrie D, McCracken JT, Sadoun T, Heinichen L, Toga AW. 2003. Cortical sulcal maps in autism. Cereb Cortex. 13:728–735.
McKinstry RC, Mathur A, Miller JH, Ozcan A, Snyder AZ, Schefft GL, Almli CR, Shiran SI, Conturo TE, Neil JJ. 2002. Radial organization of developing preterm human cerebral cortex revealed by non-invasive water diffusion anisotropy MRI. Cereb Cortex. 12:1237–1243.
Mori S, Crain BJ, Chacko VP, van Zijl PC. 1999. Three-dimensional tracking of axonal projections in the brain by magnetic resonance imaging. Ann Neurol. 45:265–269.
Nadarajah B, Alifragis P, Wong ROL, Parnavelas JG. 2003. Neuronal migration in the developing cerebral cortex: observations based on real-time imaging. Cerebral Cortex. 13:607–611.
Narr KL, Bilder RM, Kim S, Thompson PM, Szeszko P, Robinson D, Luders E, Toga AW. 2004. Abnormal gyral complexity in first-episode schizophrenia. Biol Psychiatry. 55:859–867.
Noga JT, Bartley AJ, Jones DW, Torrey EF, Weinberger DR. 1996. Cortical gyral anatomy and gross brain dimensions in monozygotic twins discordant for schizophrenia. Schizophr Res. 22:27–40.
Nowell MA, Grossman RI, Hackney DB, Zimmerman RA, Goldberg HI, Bilaniuk LT. 1988. MR imaging of white matter disease in children. Am J Radiol. 151:359–365.
Rados M, Judas M, Kostovic I. 2006. In vitro MRI of brain development. Eur J Radiol. 57:187–198.
Rakic P. 1988. Specification of cerebral cortical areas. Science. 241: 170–176.
Rapoport JL, Castellanos FX, Gogate N, Janson K, Kohler S, Nelson P. 2001. Imaging normal and abnormal brain development: new perspectives for child psychiatry. Aust N Z J Psychiatry. 35:272–281.
Retzius A. 1891. Ueber den Bau der Oberflachenschicht der Grosshirnrinde beim Menschen und bei den Saugethieren. Biologiska Foreningens Forhandlingar. 3:90–103.
Richman DP, Stewart RM, Hutchinson JW, Caviness VS, Jr. 1975. Mechanical model of brain convolutional development. Science. 189:18–21.
Sarnat HB. 1992. Regional differentiation of the human fetal ependyma: immunocytochemical markers. J Neuropathol Exp Neurol. 51:58–75.
Schmahmann JD, Pandya DN, Wang R, Dai G, D'Arceuil HE, de Crespigny AJ, Wedeen VJ. 2007. Association fibre pathways of the brain: parallel observations from diffusion spectrum imaging and autoradiography. Brain. 130:630–653.
Schmechel DE, Rakic P. 1979. A Golgi study of radial glial cells in developing monkey telencephalon: morphogenesis and transformation into astrocytes. Anat Embryol (Berl). 1979(156):115–152.
Sidman RL, Rakic P. 1973. Neuronal migration, with special reference to developing human brain: a review. Brain Res. 62:1–35.
Stagaad M, Mollgard K. 1989. The developing neuroepithelium in human embryonic and fetal brain studied with vimentin immunohistochemistry. Anat Embryol (Berl). 180:17–28.
Takahashi E, Dai G, Rosen GD, Wang R, Ohki K, Folkerth RD, Galaburda A, Wedeen VJ, Grant PE. 2011. Developing neocortex organization and connectivity in cats revealed by direct correlation of diffusion tractography and histology. Cereb Cortex. 21:200–211.
Takahashi E, Dai G, Wang R, Ohki K, Rosen GD, Galaburda A, Grant PE, Wedeen VJ. 2010. Development of cerebral fiber pathways in cats revealed by diffusion spectrum imaging. Neuroimage. 49: 1231–1240.
Takahashi E, Ohki K, Kim DS. 2007. Diffusion tensor studies dissociated two fronto-temporal pathways in the human memory system. Neuroimage. 34:827–838.
Takahashi E, Ohki K, Kim DS. 2008. Dissociated pathways for successful memory retrieval from the human parietal cortex: anatomical and functional connectivity analyses. Cereb Cortex. 18:1771–1778.
Toro R, Burnod Y. 2005. A morphogenetic model for the development of cortical convolutions. Cereb Cortex. 15:1900–1913.
Tuch DS, Reese TG, Wiegell MR, Wedeen VJ. 2003. Diffusion MRI of complex neural architecture. Neuron. 40:885–895.
Van Essen D. 1997. A tension-based theory of morphogenesis and compact wiring in the central nervous system. Nature. 385:313–318.
Van Essen DC, Dierker D, Snyder AZ, Raicle ME, Reiss AL, Korenberg J. 2006. Symmetry of cortical folding abnormalities in Williams syndrome revealed by surface-based analyses. J Neurosci. 26: 5470–5483.
Vasung L, Huang H, Jovanov-Milošević N, Pletikos M, Mori S, Kostović I. 2010. Development of axonal pathways in the human fetal fronto-limbic brain: histochemical characterization and diffusion tensor imaging. J Anat. doi: 10.1111/j.1469-7580.2010.01260.x).
Vasung L, Jovanov-Milošević N, Pletikos M, Mori S, Judaš M, Kostović I. 2011. Prominent periventricular fiber system related to ganglionic eminence and striatum in the human fetal cerebrum. Brain Struct Funct. 215:237–253.
Vishwas M, Chitnis T, Pienaar R, Healy BC, Grant PE. 2010. Tract based analysis of callosal, projection and association pathways in pediatric patients with multiple sclerosis: a preliminary study. Am J Neurodiol. 31:121–128.
Volpe JJ. 2008. Neurology of the newborn. 5 ed. Philadelphia (PA): Elsevier Science.
Wedeen VJ, Wang RP, Schmahmann JD, Benner T, Tseng WY, Dai G, Pandya DN, Hagmann P, D'Arceuil H, de Crespigny AJ. 2008. Diffusion spectrum magnetic resonance imaging (DSI) tractography of crossing fibers. Neuroimage. 41:1267–1277.
Welker W. 1990. Why does cerebral cortex fissure and fold. In: Jones EG, Peters A, editors. Cerebral cortex. New York: Plenum Press. p. 3–136.
Wilkinson M, Hume R, Strange R, Bell JE. 1990. Glial and neuronal differentiation in the human fetal brain 9-23 weeks of gestation. Neuropathol Appl Neurobiol. 16:193–204.
White T, Andreasen NC, Nopoulos P, Magnotta V. 2003. Gyrification abnormalities in childhood- and adolescent-onset schizophrenia. Biol Psychiatry. 54:418–426.
White T, Su S, Schmidt M, Kao C-Y, Sapio G. 2010. The development of gyrification in childhood and adolescence. Brain Cogn. 72:36–45.
Xu G, Knutsen AK, Dikranian K, Kroenke CD, Bayly PV, Taber LA. 2010. Axons pull on the brain, but tension does not drive cortical folding. J Biomech Eng. 132:071013.
Zilles K, Schleicher A, Langemann C, Amunts K, Morosan P, Palimero-Gallagher N, Schormann T, Mohlberg H, Bürgel U, Steinmetz H, et al. 1997. Quantitative analysis of sulci in the human cerebral cortex: development, regional heterogeneity, gender difference, asymmetry, intersubject variability, and cortical architecture. Hum Brain Mapp. 5:218–221.